Combined neutron diffraction and computer simulation study of liquid dimethyl sulphoxide

Alenka Luzar[a)]
Department of Chemistry, University of California, Berkeley, California 94720

A. K. Soper
ISIS Science Division, Rutherford Appleton Laboratory, Chilton, Didcot, Oxon, OX11 0QX, United Kingdom

David Chandler
Department of Chemistry, University of California, Berkeley, California 94720

(Received 3 May 1993; accepted 29 June 1993)

The structure of liquid dimethylsulphoxide (DMSO) at 25 °C is explored using a combination of neutron diffraction with isotope substitution and computer simulation techniques. The potentials used in the computer simulation consist of Coulomb and 6-12 Lennard-Jones interactions for each of the carbon, oxygen, and sulfur sites on the molecule. To interpret the neutron diffraction data most effectively, it is necessary to refine both the molecular internal structure *and* the intermolecular contributions to the measured structure factors at the same time in order to separate the intermolecular terms correctly, because there is a large degree of overlap between intramolecular and intermolecular distances. This renders the data far more sensitive to the intermolecular forces than if this analysis were not performed. Direct comparison of neutron diffraction data and computer simulation results indicates that existing models of the molecular force field give a sensible description of the liquid structure, although there are some discrepancies which are not fully understood at this time. The question of whether this material can be regarded as an associated liquid, as it is frequently referred to, is discussed. All tests for association that have so far been applied to both the diffraction data and the computer simulation results do not indicate a highly ordered molecular association in the liquid.

I. INTRODUCTION

We present a new study of the structure of liquid dimethylsulphoxide (DMSO) using a combination of neutron diffraction and computer simulation techniques. This study was motivated by the need to develop an effective pair potential for the DMSO molecule because of the intense interest in DMSO and its interactions with water, which have an important role in many biochemical processes.[1]

The majority of previous experimental studies on DMSO have concentrated on the DMSO–water system. For example, there are many measurements of its excess thermodynamic properties.[2–5] Other experimental techniques which have been applied include inelastic neutron scattering and x-ray diffraction,[6] infrared,[7–9] Raman scattering,[7] nuclear magnetic resonance (NMR),[10–12] dielectric measurements,[13,14] and acoustic measurements.[15–17] However, in order to establish the nature of the water–DMSO interactions, it is necessary to determine the potential for pairs of interacting DMSO molecules in the liquid state, and for this it is necessary to investigate the structure and dynamics of the pure liquid. However, the number of definitive structural studies of the pure liquid is small. Only recently have x-ray diffraction[18,19] and neutron diffraction[19] studies of the pure liquid been reported.

One of the obvious difficulties of interpreting the diffraction experiment is that there are ten distinct site–site correlation functions, with many overlapping distances both within the molecule and between molecules, and these are all added together in the measured diffraction pattern. This must lead to considerable ambiguity in determining the liquid structure directly from the diffraction data. Therefore, it is essential to employ a molecular modeling technique in order to draw any conclusions about the structure of the liquid. Both the previous studies on pure DMSO (Refs. 18 and 19) have used a similar modeling technique which starts from the structure of the crystal and considers only a rather small cluster of molecules. A particular conclusion from both experiments is that the short range molecular arrangement in the liquid apparently looks similar to the local order in the crystalline material, with the molecular dipoles of neighboring molecules lying roughly antiparallel to each other, and the methyl groups tending to cluster together. However, little information on the molecular interaction potential has so far been deduced from these data.

An alternative approach to understanding the liquid structure of DMSO is to perform a computer simulation of the liquid, using an assumed intermolecular potential. With computer simulation, one can get information on specific site–site correlations as well as determine the thermodynamic consequences of any assumed potential. The first attempt to perform model calculations was reported by

[a)]Also affiliated with Josef Stefan Institute, University of Ljubljana, Slovenia.

 0021-9606/93/99(9)/6836/12/$6.00

Rao and Singh.[20] The main goal of their work was to determine the relative differences in the free energy of solvation between the two solutes methanol and DMSO in water. Vaisman and Berkowitz[21] performed a molecular dynamics simulation of DMSO and DMSO–water mixtures. Molecular dynamics simulations including DMSO as a solvent have also been reported.[22] In both these studies,[21,22] the same intermolecular potential as in Ref. 20 was used. This potential apparently gives a fair agreement with the existing structural data[18,19] as far as pair distances are concerned, although given the likely ambiguities of assigning definite atom–atom distances directly from the experimental data, it is not clear that comparing the simulation with the diffraction experiment in this way is reliable. At the same time, this same potential does not predict thermodynamic properties accurately. Specifically, the calculated mean potential energy is 30% lower than the reported experimental value.[1,23]

Recently, we have used two different force field models to study concentrated DMSO–water solutions by molecular dynamics computer simulation.[24] The results of those simulations were shown to compare well with our recent neutron diffraction experimental data using hydrogen isotope substitution,[25] Even for the highly concentrated 1DMSO:2H_2O solution, the water hydrogen–hydrogen radial distribution function $g_{HH}(r)$ exhibited the characteristic tetrahedral ordering of water–water hydrogen bonds. With either potential model (denoted *P*1 and *P*2 in Ref. 24), our molecular dynamics results drew a microscopic picture of hydrogen bonding in water–DMSO mixtures which was largely invariant to the details of the intermolecular pair potential of DMSO. In particular, in the mixing process, hydrogen bonding was simply transferred from water–water interactions to water–DMSO interactions. This picture is also in accord with the qualitative ideas underlying the mean field model of hydrogen bonding mixtures.[26–28] However, we could not give preference to either of the two force field models on the basis of the water pair correlation functions in the mixture alone.

The present work attempts to make a more comprehensive test of several proposed intermolecular potential models for DMSO than has been achieved before. In the first place, some thermodynamic and electrostatic properties associated with each proposed potential are evaluated and compared with known experimental values. Second, we have performed, for the first time on pure DMSO, hydrogen isotope substitution on the methyl hydrogen atoms in order to provide more precise information about specific site–site correlations from the neutron diffraction experiment. Finally, given that the experimental pair correlation functions are for the most part weighted sums of several partial functions, we make a direct comparison of simulation with experiment by showing both experimental and theoretical pair correlation functions and composite structure factors, evaluated with the same weighting coefficients as in the neutron experiment. This comparison has not so far been made in any of the previous work on DMSO.

The paper is organized as follows: The neutron diffraction experiment is described and results reported in Sec. II. The computer simulation is described in Sec. III and the two are compared and discussed in Sec. IV. Finally, our conclusions are summarized in the last section, where the consequences of the present results for future investigations are also reviewed.

II. NEUTRON DIFFRACTION EXPERIMENT

A. Analysis procedures

A full description of the neutron diffraction experiment has already been given for the case of solutions of DMSO in water,[25] and since the methods used to analyze the data from the pure DMSO were identical to those used before, only a summary is given here.

The useful quantity extracted from the diffraction data is the total interference function $F(Q)$, which is a neutron weighted sum of partial structure factors (PSFs) $H_{\alpha\beta}(Q)$. These partial structure factors are in turn related by Fourier transform to the corresponding site–site pair correlation functions $g_{\alpha\beta}(r)$,

$$H_{\alpha\beta}(Q)=4\pi\rho\int_0^\infty r^2[g_{\alpha\beta}(r)-1]\frac{\sin Qr}{Qr}dr, \tag{1}$$

where ρ is the atomic number density for the material in question.

In principle, the partial structure factors can be obtained by combining diffraction data from several experiments with different isotopes of the constituent atoms, but for DMSO, only the hydrogen and sulfur atoms present a feasible diffraction contrast for neutrons. This experiment used hydrogen isotopes on the methyl hydrogens on the DMSO molecule—one experiment was with the methyl hydrogens fully protonated, another with methyl hydrogens fully deuterated, and a third was a 64:36 molar ratio mixture of the first two samples, the last sample corresponding to a mixture with zero coherent scattering length for intermolecular interactions involving hydrogen atoms ($b_H=-3.74$ fm, $b_D=6.67$ fm).

In cases such as these, where a full separation of the partial structure factors is not possible, the isotopic contrasts still lead to useful interatomic information on the structure of both the DMSO molecules themselves and on the liquid they form. The total interference cross section can be split into three composite partial structure factors (CPSFs)—hydrogen to hydrogen H_{HH}, unlabeled atoms to hydrogen H_{XH}, and unlabeled to unlabeled H_{XX} (X=S, C, O). The total interference structure factor is then expressed in terms of these CPSFs as

$$F(Q)=c_X^2b_X^2H_{XX}+2c_Xc_Hb_Xb_HH_{XH}+c_H^2b_H^2H_{HH}, \tag{2}$$

where

$$b_X=\sum_{\alpha\neq H}c_\alpha b_\alpha \Big/ c_X \tag{3}$$

$$c_X=\sum_{\alpha\neq H}c_\alpha, \tag{4}$$

and $c_H=(1-c_X)$ is the combined atomic fraction of all distinct hydrogen sites on which substitutions are made. It

should be noted that, in general, the composite partial structure factors defined in this way include the *intra*molecular correlations as well as intermolecular correlations. However, because the methyl hydrogens do not exchange with hydrogen atoms on other molecules of DMSO, the HH partial structure factor obtained from the isotope substitution experiment will *not* contain any intramolecular contributions. These HH *intra*molecular contributions then appear as additional terms in the XH and XX CPSFs. Thus the latter two CPSFs are represented as neutron weighted averages of several *inter*molecular PSFs, plus the corresponding *intra*molecular term, plus a term relating to the H–H intramolecular correlations

$$H_{\mathrm{XH}}=\sum_{\alpha\neq H}\frac{c_\alpha b_\alpha}{c_{\mathrm{X}}b_{\mathrm{X}}}H_{\alpha H}^{\mathrm{inter}}+\sum_{\alpha\neq H}\frac{b_\alpha}{2N_m c_{\mathrm{X}}b_{\mathrm{X}}}H_{\alpha\mathrm{H}}^{\mathrm{intra}}+\frac{(b_{\mathrm{D}}+b_{\mathrm{H}})}{2N_m c_{\mathrm{X}}b_{\mathrm{X}}}H_{\mathrm{HH}}^{\mathrm{intra}},\tag{5}$$

$$H_{\mathrm{XX}}=\sum_{\alpha\neq H,\beta\neq H}\frac{c_\alpha c_\beta b_\alpha b_\beta}{c_{\mathrm{X}}^2 b_{\mathrm{X}}^2}H_{\alpha\beta}^{\mathrm{inter}}+\sum_{\alpha\neq H,\beta\neq H}\frac{b_\alpha b_\beta}{N_m c_{\mathrm{X}}^2 b_{\mathrm{X}}^2}H_{\alpha\beta}^{\mathrm{intra}}-\frac{(b_{\mathrm{D}}b_{\mathrm{H}})}{N_m c_{\mathrm{X}}^2 b_{\mathrm{X}}^2}H_{\mathrm{HH}}^{\mathrm{intra}},\tag{6}$$

where N_m is the number of atoms in the DMSO molecule ($N_m=10$) and throughout it is assumed that all structure factors are defined as per atom of liquid. Here the intramolecular term $H_{\alpha\beta}^{\mathrm{intra}}$ is defined as

$$H_{\alpha\beta}^{\mathrm{intra}}(Q)=\sum_{i=\alpha,\ j=\beta}{}'\frac{\sin Q r_{ij}}{Q r_{ij}}\exp\left(\frac{-Q^2\sigma_{ij}^2}{2}\right),\tag{7}$$

where the prime indicates that the summation is taken *only* over atoms in the same molecule and r_{ij} is the average separation of the ith and jth atoms of type α and β, respectively, in the molecule. The standard deviation of this distance is given by σ_{ij}, and this formula assumes that the atoms have a Gaussian distribution about this average distance.

The third CPSF H_{HH} consists only of the *inter*molecular correlation between methyl protons.

B. Results of neutron diffraction experiment

As in the previous experiment on DMSO–water solutions,[25] the neutron data were collected on the small angle neutron diffractometer for amorphous and liquid samples (SANDALS) at the ISIS Pulsed Neutron Source, United Kingdom. This is a high count rate diffractometer which minimizes the distortions in the diffraction data introduced by nuclear recoil in the scattering process by concentrating all its detectors at low scattering angles. All three samples (fully deuterated DMSO, fully protonated DMSO, and a 36 mol % D:64 mol % H mixture of these liquids) were contained in the same 1 mm thick flat plate zirconium–titanium alloy container, similar to the ones used before. The subsequent data analysis steps were identical to those used before.

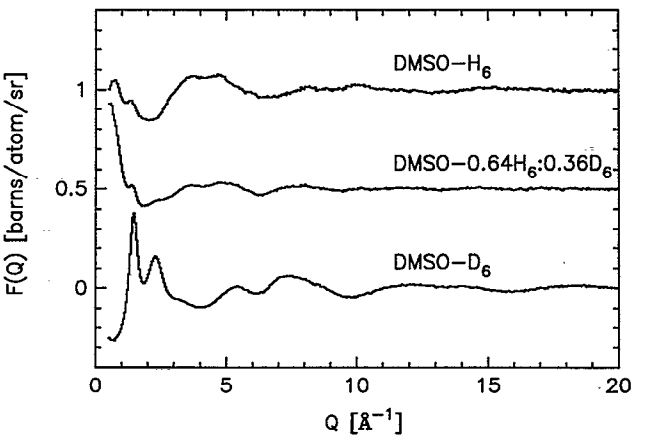

FIG. 1. Measured differential interference cross sections for pure DMSO at 25 °C for protonated DMSO (top, shifted 1b/atom/sr upwards), deuterated DMSO (bottom), and a 64:36 mol % (middle, shifted 0.5b/atom/sr upwards).

The three total interference functions that were obtained in this experiment are shown in Fig. 1 and the total composite partial structure factors that result from these are shown in Fig 2. The diffraction data from the fully deuterated DMSO which appear in Fig. 1 look very similar to what has been measured before.[19] It will be readily apparent, however, that as they stand, it is not easy to draw any obvious conclusions from these data. Table I lists the relative weights of the various intermolecular partial structure factors which appear in Eqs. (5) and (6), while Table II lists the corresponding intramolecular weightings.

The next step in the data analysis was to estimate the structure of the molecule from the data. To do this, the atomic coordinates were set up to correspond to those found in the crystalline state.[29,30] The atoms were then allowed to move in random amounts over a range ±0.1 Å about the crystal values. At the same time, the methyl groups were allowed to rotate in random amounts about

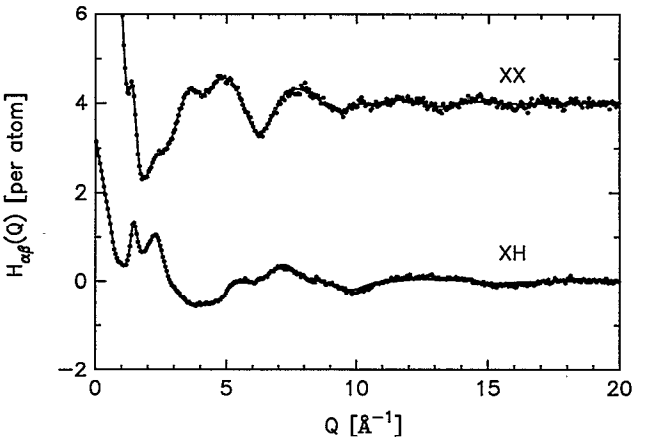

FIG. 2. Measured composite partial structure factors (points) for DMSO for XX (top, shifted upwards by 4) and XH (bottom). The solid lines correspond to fits to the data obtained by a joint refinement of the intramolecular form factor and the intermolecular correlation functions.

TABLE I. Intermolecular neutron weighting factors for individual terms in the composite partial structure factors from pure DMSO liquid. The weighting for a particular atom pair is obtained by looking along the appropriate row and column for that pair.

	S	O	C
XX composite partial structure factor			
S	0.0167		
O	0.0684	0.0700	
C	0.1566	0.3208	0.3675
XH composite partial structure factor			
H	0.1292	0.2646	0.6063

the carbon–sulfur bond. For each new position, the $H_{\alpha\beta}^{\text{intra}}$ were calculated according to Eq. (7). The standard deviations assumed for this model were derived from the equation

$$\sigma_{ij}=\sigma_1+\sqrt{r_{ij}}\sigma_2 \tag{8}$$

with two effective width parameters σ_1 and σ_2, which were refined alongside the atomic coordinates. It was felt that given the high degree of overlap of intramolecular distances, there was little to be gained in attempting to refine the individual σ_{ij}'s. At the same time, the *inter*molecular pair correlation functions were estimated using the minimum noise method (MIN)[31] which was used in the previous study of DMSO–water mixtures. Another description of this method has appeared recently.[32] The combined intermolecular and intramolecular structure factors were then compared to the measured CPSFs via the χ^2 statistic, and accepted or rejected using standard Metropolis Monte Carlo rules. Thus the molecular structure was refined *at the same time* as the intermolecular correlations, a procedure which is rarely adopted when analyzing data from molecular liquids. However, it is essential to use such a procedure in the case of DMSO because of the large degree of overlap between the intramolecular and intermolecular correlations. This molecular refinement was carried out separately for the XX and XH structure factors. The fits to these two CPSFs are shown as the solid lines in Fig. 2.

Table III gives a list of some of the refined molecular distances from the XX refinement and Fig. 3 shows a perspective view of the refined molecule. The structure obtained from the refinement of the XH data was not tangibly different, except that the orientation of the methyl groups was slightly different. However, the weighting of the HH intramolecular correlation in the XH function is much weaker than in the XX function, so we believe the structure derived from the XX data is more reliable. In particular, it was found that although the refinement allowed random rotations of the methyl groups, most of those rotations were rejected, and the two methyl groups adopted quite definite relative orientations. This does not mean that the methyl groups are not free to rotate, but simply that

TABLE II. Neutron weightings on individual intramolecular atom–atom contributions to the total composite partial structure factors.

XX composite partial structure factor		
S	O	0.342
S	C	0.392
O	C	0.802
C	C	0.919
H	H	0.518
XH composite partial structure factor		
S	H	0.108
O	H	0.220
C	H	0.253
H	H	0.111

TABLE III. Refined molecular parameters derived from the XX composite partial structure factor in liquid DMSO (except the C–H bond distance which is obtained from the XH CPSF. (A) Average intramolecular distances and their standard deviations in Ångstroms. For the OH distances, the three average values are shown in order of increasing distance. (B) Average fitted bond angles. The uncertainties on these are hard to estimate, but are thought to be on the order of 2°. (C) See Eq. (8).

(A)	S	O	1.526±0.006
	S	C	1.738±0.025
	O	C	2.736±0.016
	C	C	2.648±0.010
	S	H	2.421±0.053
	O	H_1	2.84 ±0.12
	O	H_2	3.17 ±0.10
	O	H_3	3.75 ±0.03
	C	H	1.10 ±0.07
(B)	∠OSC=114°		∠CSC=99°
(C) σ_1=0.067 Å, σ_2=0.047 (Å)$^{1/2}$			

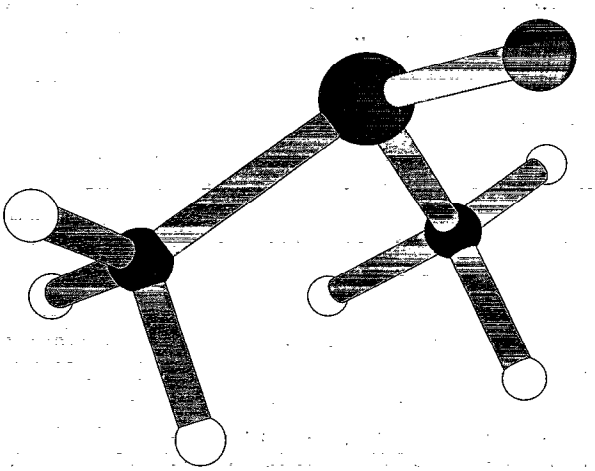

FIG. 3. A perspective view of the DMSO molecule obtained from the fit to the XX data. The fit to the XH data yielded essentially the same structure. The large atom in the center is the sulfur atom. Attached to this are two carbon atoms (black) and an oxygen atom (lighter). The three smaller atoms attached to each carbon are the methyl hydrogens. It was found that these do not adopt random rotations around the C–S bond, but probably rotate in jumps around the positions shown here.

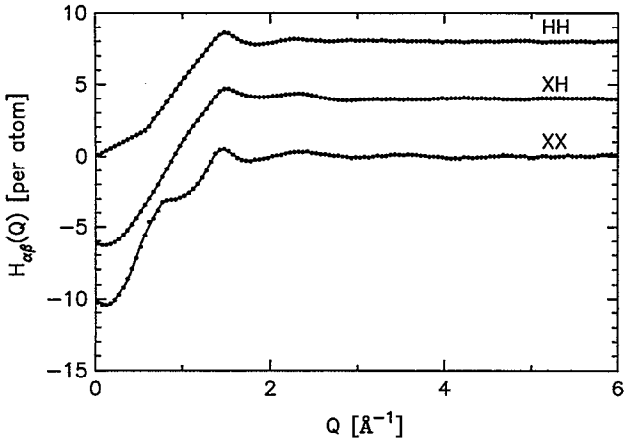

FIG. 4. Measured intermolecular composite partial structure factors. HH (top, shifted upwards by 8) is obtained directly from the data of Fig. 1, while XH (middle, shifted upwards by 4) and XX (bottom) are obtained from the data of Fig. 2 after subtracting the intramolecular form factors. The solid lines show the fit to the data obtained in the refinement of the intermolecular correlation functions.

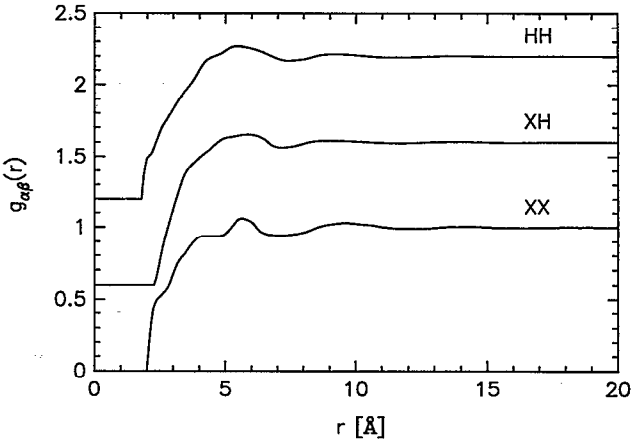

FIG. 5. Intermolecular composite pair distributions derived from the data of Fig. 4.

they apparently do not undertake free rotation and instead rotate in jumps about three equivalent sites.

In general, the molecular structure is very similar to what has been seen in many previous determinations in both the liquid and crystal.[18,19,29,30] The only significant discrepancy is the OSC bond angle, which is about 6° larger than what has been found previously. It arises from the somewhat larger O–C distance found in these data. Unfortunately, this distance overlaps quite closely with the C–C distance and some H–H distances, making its precise determination somewhat uncertain. Within these likely uncertainties, we believe the molecule is not significantly different to what has been seen in the crystalline state. However, none of the previous studies apparently allude to the problems of distinguishing between overlapping distances, nor give any indication of the uncertainty in the molecular structure that this introduces.

The residue from subtracting the refined molecule structure from the partial structure data gives the intermolecular CPSFs, which are the most interesting from the point of view of understanding the intermolecular interaction potential. The intermolecular functions determined in this experiment are shown in Fig. 4 and the corresponding pair correlation functions which are derived from them are shown in Fig. 5.

Not surprisingly, the amplitude of the structural oscillations decreases somewhat in going from XX to HH correlation, but it is quite noticeable that qualitatively the three functions look remarkably similar, with a broad peak centered near 5 Å and a series of decaying oscillations out to ~20 Å, even though the hydrogens on the molecule are in quite distinct positions compared to the other atoms (see Fig. 3). The 5 Å peak in the XX function is apparently split, with a shoulder near 4 Å on the low r side. This trend in the three composite structure factors compares quite dramatically with liquids known to be hydrogen bonded such as water, where the HH, OH, and OO correlation functions have quite different and distinctive forms. Hence, on this simple analysis of the correlation functions determined from the diffraction data, DMSO appears much less associated than water. Two recent interpretations[20,21] of the previous diffraction data[18,19] have implied there might be weak hydrogen bonds in the liquid, but the lack of any signature of such interactions in the HH and XH distributions confirms the generally accepted view that DMSO cannot be hydrogen bonded.[6,9]

III. COMPUTER SIMULATIONS

A. Intermolecular potentials

In seeking to describe the interactions between DMSO molecules, we have made several simplifying assumptions. First, we have treated the molecules as rigid objects, with bond lengths and angles taken from the crystallographic structure[29] $r_{SO}=1.53$ Å, $r_{SC}=1.8$ Å, $\angle OSC=106.75°$, and $\angle CSC=97.4°$. We further suppose that the electrostatic contribution to the intermolecular potential may be adequately represented by fractional charges placed at the atomic sites. Polarizability and concommittant many-body interactions are ignored. Finally, we assume that the short range interaction can be described by a set of atom–atom potentials of the Lennard-Jones type, characterized by the usual energy and distance parameters $\epsilon_{\alpha\beta}$ and $\sigma_{\alpha\beta}$ with $\alpha,\beta=C_1$, C_2, S, and O. With these assumptions, the energy of interaction is

$$U_{\alpha\beta}(r)=\frac{q_\alpha q_\beta}{r}+4\epsilon_{\alpha\beta}\left[\left(\frac{\sigma_{\alpha\beta}}{r}\right)^{12}-\left(\frac{\sigma_{\alpha\beta}}{r}\right)^{6}\right], \tag{9}$$

where q_α and q_β are the fractional charges in units of $|e|$ and the cross interaction parameters are determined by the usual mixing rules

$$\epsilon_{\alpha\beta}=(\epsilon_{\alpha\alpha}\epsilon_{\beta\beta})^{1/2},\quad \sigma_{\alpha\beta}=\tfrac{1}{2}(\sigma_{\alpha\alpha}+\sigma_{\beta\beta}). \tag{10}$$

First, we have simplified the calculations using a four site model only by replacing the methyl group carbon and hydrogen interaction sites by a single site (CH_3) located on the methyl carbon atom. Later, when we make compari-

TABLE IV. Intermolecular potential parameters.

	ϵ (kJ mol^{-1})	σ (Å)	q ($P1$)	q ($P2$)
	$P1$ and $P2$ potentials			
Oxygen	0.29922	2.80	−0.54	−0.459
Sulfur	0.99741	3.40	0.54	0.139
Methyl group	1.230	3.80	0.0	0.160
	RS potential[a]			
	ϵ (kJ mol^{-1})	σ (Å)	q	
Oxygen	0.276144	2.94	−0.459	
Sulfur	0.845168	3.56	0.139	
Methyl group	0.66999	3.60	0.160	

[a]Reference 20.

sons with neutron diffraction data, we obtain $g_{HH}(r)$ and $g_{XH}(r)$ by taking into account all the hydrogen atoms geometrically, but they are not present in the Hamiltonian. The resulting four site model involves nine adjustable parameters—three independent charges q_α, with $\Sigma_\alpha q_\alpha = 0$; three characteristic energies $\epsilon_{\alpha\alpha}$, and three characteristic lengths $\sigma_{\alpha\alpha}$.

The Lennard-Jones interaction coefficients and charges were chosen on the basis of experimentation with ~50 simulation runs, using as criteria accurate values of the experimental heat of vaporization,[23] vanishing pressure, and charge distribution leading to a dipole moment at least as big as that of the gas phase molecule [$\mu_g \sim 4$ D (Ref. 33)].

We present two potentials which fulfill these criteria. We call them $P1$ and $P2$ to be consistent with Ref. 24. The Lennard-Jones parameters in $P1$ and $P2$ for O, S, and CH_3 are those of the isoelectronic Ne, Ar, and CH_4, respectively. The $P1$ potential has no charges on the methyl groups and a positive and negative charge on sulphur and oxygen atoms. This kind of charge distribution gives the dipole moment $\mu_g = 4$ D, which would be localized along the S–O bond as indicated by experimental data.[33,34] In the $P2$ potential, we used the same partial point charges as those used by Rao and Singh.[20] Those charges were obtained by fitting the electrostatic potential around the DMSO molecule to a point charge model.[35] The electrostatic potential of the molecule was obtained by an *ab initio* method with 6-31G* basis set.[36] This charge distribution gives the dipole moment of 4.3 D. Rao and Singh's (RS) potential differs from the $P2$ potential in the choice of Lennard–Jones parameters. All the Lennard-Jones parameters and the fractional charges for the three different force field models $P1$, $P2$, and RS are listed in Table IV. Our molecular dynamics results for the mean potential energy per mole $\langle U \rangle$ and pressure are listed in Table V. Both potentials $P1$ and $P2$ give good agreement with the experimental estimate of the mean potential energy per mole $\langle U \rangle_{exp}$. The mean potential energy obtained from the RS potential[20] is on the other hand 30% lower than the reported experimental value.[23]

TABLE V. Molecular dynamics results for liquid DMSO—the mean potential energy per mole $\langle U \rangle$ and pressure P using different force fields. The experimental estimate of the mean potential energy per mol $\langle U \rangle_{exp} = -50.49 \pm 0.42$ kJ mol^{-1} was obtained by subtracting $PV \sim RT$ from the measured enthalpy of vaporization (Ref. 23).

Force field model	$\langle U \rangle$ (kJ mol^{-1})	P (kbar)
$P1$	−53.96±0.22	0.34±0.19
$P2$	−49.00±0.29	−0.07±0.26
RS	−36.22±0.26	0.08±0.21

B. Molecular dynamics calculations

The technical details of the molecular dynamics simulations were similar to those in our earlier work on DMSO–water mixtures.[24] The high temperature run was started from a cubic lattice arrangement of molecules and the final configuration from this calculation was used to initiate the low temperature run. The calculations were carried out in the N, V, T ensemble, and the Nosé–Hoover thermostat[37,38] was used to control the temperature at 298 K. In a system of 432 DMSO molecules, the root mean square fluctuations in the temperature were 7–8 K. With the thermostat off, a time step of 0.5 and/or 1 fs conserved energy adequately. The drift in energy was 0.0025 kJ/mol per picosecond, representing only 0.005% of the total energy. The equations of motion were integrated using the velocity predictor–corrector method. The long range electrostatic interactions were treated using the Ewald summation technique.[39] Periodic boundary conditions were used together with the minimum image convention for non-Coulombic interactions.[39] Both the energy and pressure have been corrected for the effect of truncating the Lennard-Jones potentials at one-half of the simulation box length. The most important technical data are collected in Table VI. The simulation runs were performed on both a Cray XMP/416 and an IBM/RS 6000.

C. Results of computer simulations

The six atom–atom distribution functions obtained from the simulation for the $P1$, $P2$, and RS potentials are shown in Figs. 6(a)–6(f).[40] All the pair correlation functions for those potentials which have the same distribution of charges, namely $P2$ and RS, look very similar, except for $g_{CC}(r)$. Recall, that the Lennard-Jones ϵ_{CC} parameter in the RS potential is approximately two times smaller than

TABLE VI. Technical features of the molecular dynamics (MD) simulations of liquid DMSO.

Force field model	Number of molecules	Temperature (K)	Integration step (ps)	Total time of simulation (ps)	MD box size[a] (Å)
$P1$	432	298	0.0005	70	36.76
$P2$	250	298	0.001	160	18.38
RS	250	298	0.001	40	18.38

[a]Determined from the experimental density of DMSO at room temperature (Ref. 2).

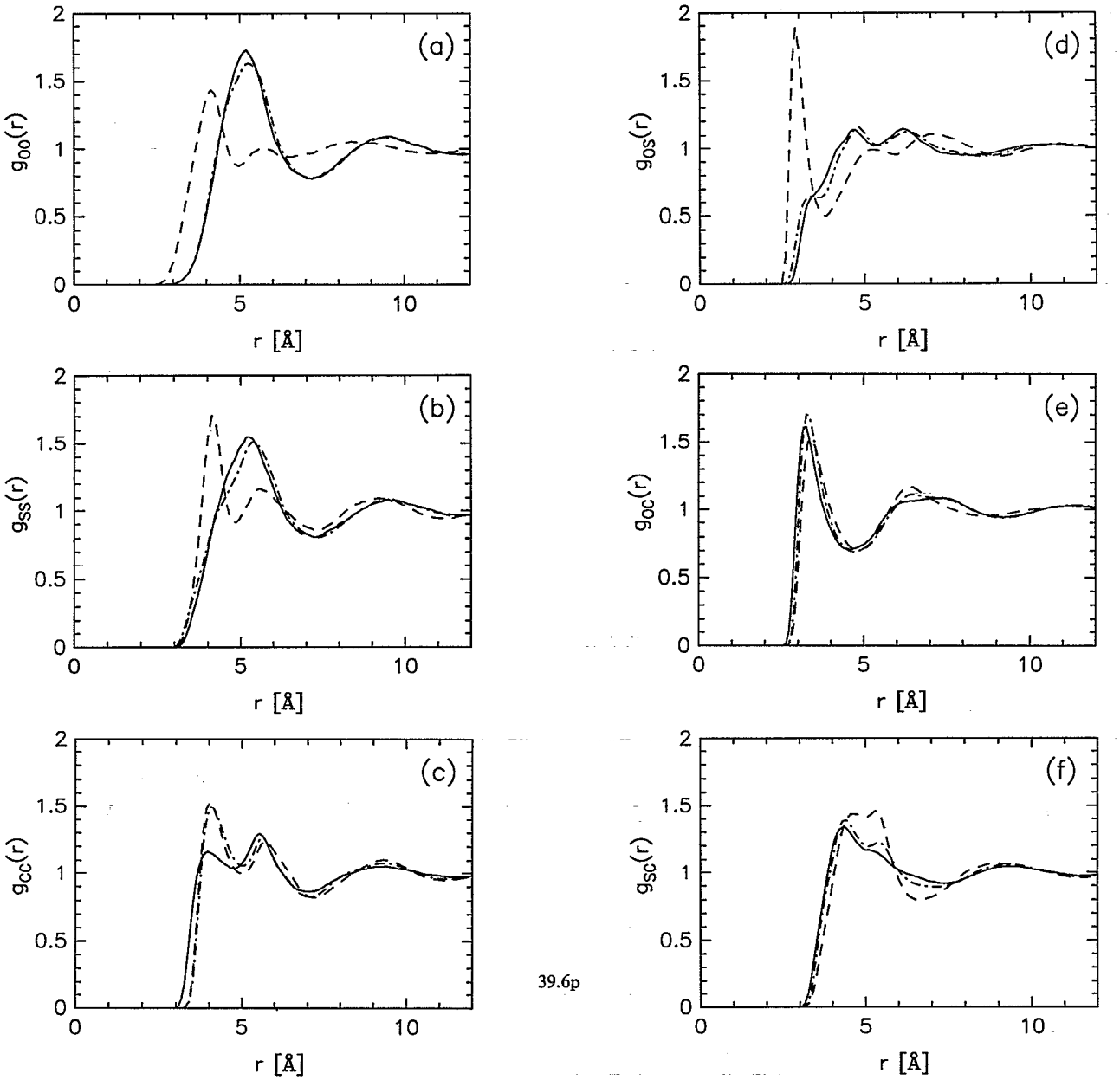

FIG. 6. A comparison of (a) O–O; (b) S–S; (c) C–C; (d) O–S; (e) O–C; and (f) S–C atom–atom pair correlation functions for the three potentials RS (line), *P*1 (dashed), and *P*2 (dotted–dashed).

the same energy parameter in the *P*2 force field model. For all three potentials *P*1, *P*2, and RS, we observe the first peak in $g_{SS}(r)$ and $g_{OO}(r)$ at the same position. Integrating these radial distribution functions out to 7.1 Å, which is the position of the first minimum in the SS and OO correlations for the *P*2 and RS potentials, a coordination number of approximately 12 molecules is obtained for both oxygen and sulfur atoms. Furthermore, for all three force field models, we find about three methyl groups around an oxygen atom by integrating $g_{OC}(r)$ out to 4.8 Å. The *P*1 potential, which has zero charge on the CH_3 groups, naturally gives very different atom–atom pair distribution functions for S–S, O–S, and O–O interactions. In particular, while we observe a broad peak with two maxima in $g_{OS}(r)$ for the *P*2 and RS potentials, a single sharp peak at 2.9 Å is observed for the *P*1 potential.

IV. A COMPARISON OF NEUTRON EXPERIMENT AND COMPUTER SIMULATION

In the previous two sections, we have shown separately the results of the neutron diffraction experiment and those of the computer simulation. From the experimental point of view, it is probably fair to say that of the three composite partial structure factors, the HH function is the most reliable because it can be extracted from the measured differ-

ential scattering cross sections with the least number of approximations,[41,42] and in the case of DMSO, contains no intramolecular correlations. On the other hand, the XX pair correlation function has more structure than the HH pair correlation function and is therefore the most useful for comparing the diffraction and computer simulation results. Therefore, given the fact that the intramolecular correlations extracted from the experimental XX CPSFs are in fact in good agreement with what has been reported before (see Fig. 3 and Table III), we have used the intermolecular XX pair distribution for the primary comparison between simulation and experiment.

A. XX correlations

Figures 7(a)–7(c) show the pair correlation function $g_{XX}(r)$ derived from the experimental XX CPSFs together with the same function calculated from simulations with each of the three potentials described here, using the same neutron weights as occur in the experiment. The $g_{XX}(r)$ distribution function is dominated by C–C and C–O correlations, and to a lesser extent, by the S–C correlation (see Table I). The S–S, S–O, and O–O partial correlation functions on the other hand make a relatively weak contribution to the $g_{XX}(r)$ function, so it is difficult to draw conclusions about these correlations. It can be seen that there is overall agreement with experiment in the shape of the simulated curves, as regards both positions and heights of peaks, particularly for r values >6 Å. The position of the 5.6 Å peak is reproduced correctly by all three potentials, as are also the subsequent larger r oscillations.

The greatest discrepancy between experiment and simulation occurs for $r<5$ Å for all three potentials. The RS potential apparently shows the best short range agreement with experiment. However, the mean potential energy for this force field model is 30% below the measured value for DMSO (Table V). Therefore, it appears that none of the present potentials give a complete account of the short range molecular interactions. The *P*2 potential gives a reasonable representation of the experimental correlation function and this potential also generates the correct experimental mean potential energy. Of the three, the *P*1 potential shows the worst agreement with the experimental correlation functions.

An alternative way to compare the simulation with experiment is to use the simulated pair correlation functions to estimate the XX composite partial structure factors and compare them with the measured data in Q space. For this representation, the intermolecular $g_{XX}(r)$'s were fixed at their simulated values and the intramolecular parameters refined to give the best fit to the total CPSFs of Fig. 2. The comparison is shown in Figs. 8(a)–8(c) for the same three potentials.

It is apparent that the correlations generated by all three potentials look similar when transformed into Q space. The distinctions between them and the experimental data follow the same trend as was seen in r space, but are much less obvious because of the intramolecular form factors, which dominate the diffraction pattern in this case. The *P*1 potential again shows worst agreement with the experiment, but there is only a small distinction between the *P*2 and RS potentials.

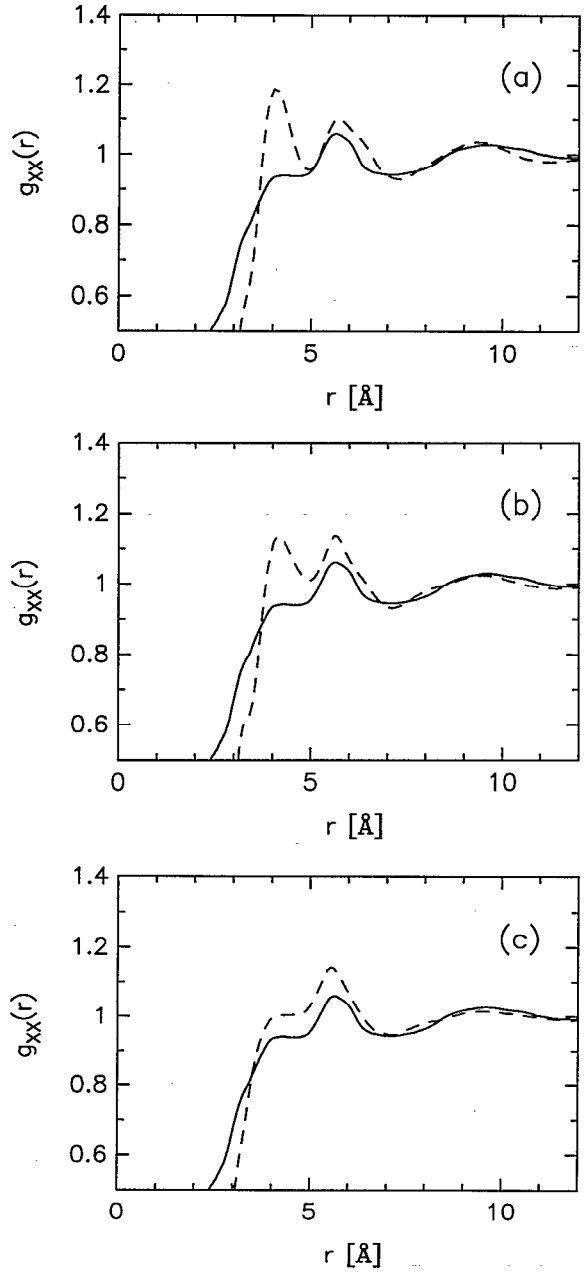

FIG. 7. A comparison of experimental $g_{XX}(r)$ (line) with the simulation results from the three potentials (a) *P*1; (b) *P*2; and (c) RS. The atom–atom correlation functions of Fig. 6 have been combined with the same weightings as occur in the neutron experiment (Table I.)

B. XH and HH correlations

To obtain the XH and HH radial distribution functions by computer simulation, we performed two short simulation runs with the two force field models *P*2 and RS, i.e., those which gave better agreement with the neutron diffraction data on the basis of comparison with the g_{XX} function. In those calculations, we included the positions of all six hydrogens on methyl groups of the DMSO molecule, but not their interaction with other atoms. The C–H

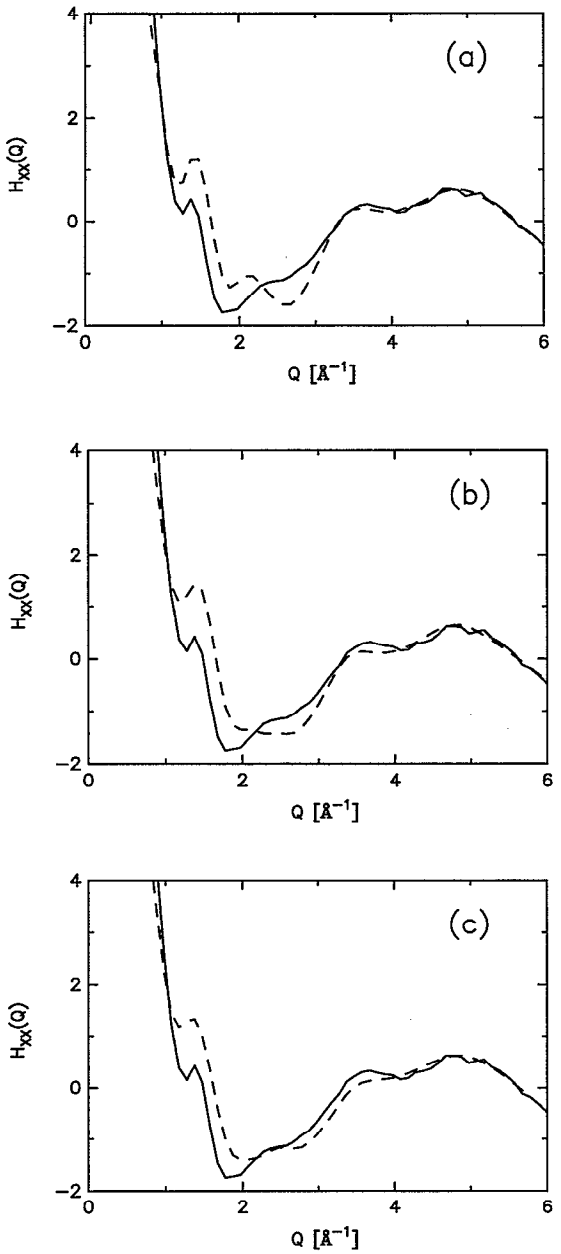

FIG. 8. A comparison of experimental total composite partial structure factors $H_{XX}(r)$ (line) with the simulation results of the three potentials (a) $P1$; (b) $P2$; and (c) RS. To make this comparison, the simulated $g_{XX}(r)$ functions of Fig. 7 were transformed to Q space and then the molecular form factor refined and added to the simulated intermolecular terms.

bond length ($r_{CH}=1.08$ Å) and the angle ∠HCH ($=109.47°$) were taken from the crystallographic structure.[29] The simulation with the $P2$ potential was performed for another 12 ps and the one with the RS potential for another 7 ps, starting from the final configurations of the runs reported in Table VI.

In Figs. 9 and 10, we make a direct comparison of the XH and HH pair correlation functions obtained from the simulation of liquid DMSO with those obtained from the experiment. It can be seen that on the basis of these correlations, there is no significant difference between the two

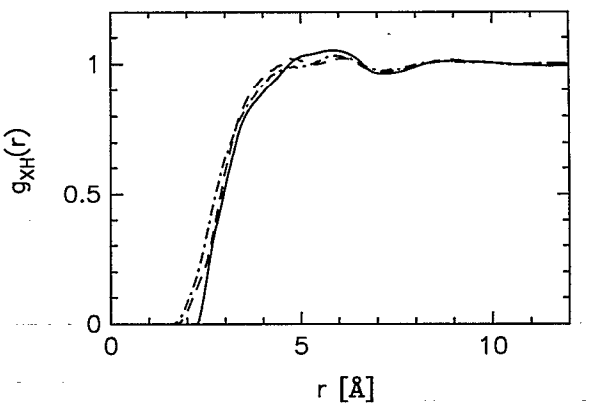

FIG. 9. A comparison of experimental XH correlation function (line) with simulated results $P2$ (dashed) and RS (dotted–dashed). To make this comparison, the hydrogen atoms were given the same positions in the molecule as were found from crystallography (Ref. 29), but there were no interaction sites located on the hydrogen atoms.

potentials. However, what is remarkable about these correlations is their general similarity in shape to the g_{XX} functions. In contrast, for the case of water, the g_{OH} and g_{HH} correlation functions both show two well-defined intermolecular peaks. These two peaks are, however, at quite distinct r values and relate to the molecular geometry of the water molecule and the presence of hydrogen bonds and to the tetrahedral short range order in the liquid. For DMSO, there are six hydrogens instead of the two for water, but even with the smearing effect of these six hydrogen atoms, their positions in the DMSO molecule are sufficiently asymmetric (see Fig. 3) that if there were a high degree directionality between the molecules, then this would show up in the XH and HH correlation functions as distinct low-r peaks or shoulders. It does seem evident that pronounced directional intermolecular correlations do not occur in DMSO liquid.

C. Discussion

In both previous simulation studies of the liquid DMSO, using the RS force field model,[20,21] it was pointed

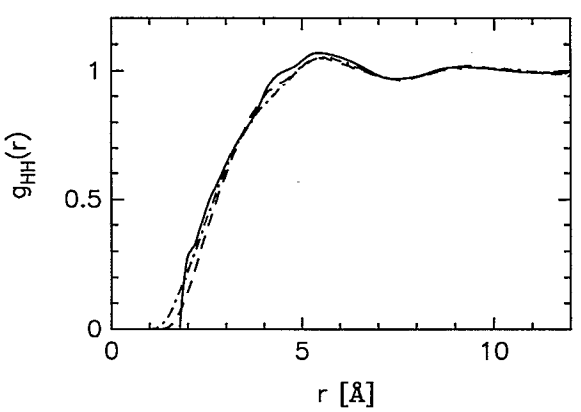

FIG. 10. A comparison of experimental HH correlation function (line) with the simulated results (the same notation as Fig. 9).

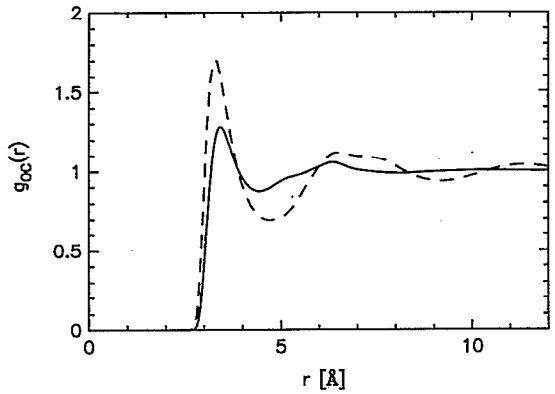

FIG. 11. The effect of atomic site charges on the O–C correlations. The simulated O–C correlation obtained from the *P*2 potential (dashed line) is compared with the same correlation obtained via the RISM integral equation approach (solid line) using the same repulsive Lennard-Jones parameters, but with all the charge and attractive interactions switched off. Although somewhat weaker, the near-neighbor peak is still quite pronounced in the RISM calculation, but the longer range oscillations are much weaker than when the charge interactions and the attractive part of the Lennard-Jones are included.

out that the first peak in the radial distribution function of the C–O pair, which is the shortest intermolecular pair distance, is sharper than the peaks for the other pairs. On the basis of this observation alone, a suggestion was made[20,21] that the DMSO molecules are linked through some weak hydrogen bonds between the oxygen atom and the methyl hydrogens. It is claimed that this is consistent with distances obtained from the x-ray diffraction data.[18,19] However, the x-ray distances depended heavily on modeling a small cluster of molecules and could be quite unreliable for reasons of ambiguity as already discussed in the Introduction. We observe this same strong short ranged peak with both potentials *P*1 and *P*2 [Fig. 6(e)] in addition to the RS potential. Bearing in mind that the *P*1 potential has no charges on the methyl groups, we cannot assume that a pronounced peak in g_{OC} corresponds solely to the effects of molecular association.

In fact, a sharp peak in g_{OC} is found in purely packing models, where association is manifestly absent. To show this, we have studied the effects of the short range repulsive forces as described approximately by the Weeks–Chandler–Andersen (WCA) repulsive part of the Lennard-Jones potential,[43] removing all other interactions. For this model, we have solved the reference interaction site model (RISM) integral equation[44] using Percus–Yevick (PY) closure. For the OC corrrelations, a similar peak to that observed in the simulation using the full potential [Eq. (9)] can be observed in the g_{OC} pair distribution function even when no charges are present on any atoms. Figure 11 compares the g_{OC} pair distribution function obtained from the simulation using the *P*2 potential with the RISM calculation using the same Lennard-Jones parameters as the *P*2 potential, but no charges. The peak is about the same width as when charges are present, although it has a lower amplitude. The indications are therefore that packing forces can give rise to at least part of the pronounced C–O intermolecular short range interaction seen in the simulation with the full potential.

Other evidence which tends to argue against a high degree of molecular association is the near-neighbor coordination number in the liquid. Previously we showed that the coordination number derived from the SS and OO partial correlation functions corresponds to about 12 near-neighbor DMSO molecules. The same number is obtained if the experimental XX correlation function is integrated out to the first minimum at $r=7.2$ Å. These numbers are those characteristic of a tightly packed nonassociated liquid.

This is not to say that the molecular charges do not play an important role in structuring the liquid. It can be seen from Fig. 11 that there are discrepancies, particularly at larger r values, between the purely repulsive force model and the simulated results. Therefore, it is unlikely that the measured correlation functions can be explained by the packing forces of the Lennard-Jones cores alone.

Yet another indicator which can be used to discuss the degree of association in the liquid is the Kirkwood correlation factor $g_1=1+\langle(N-1)\mathbf{u}_1\cdot\mathbf{u}_2\rangle$, which is a measure of the orientational correlation of the molecular dipoles,[45–47] $\mathbf{u}_i$ is a unit vector in the ith molecule of the N molecule system. For DMSO, the g_1 factor at 25 °C is essentially unity, the uncorrelated value.[48,49] This is to be contrasted with the value of 2.9 for water at the same temperature,[49] where powerful short ranged hydrogen bond forces produce specific orientational correlations and a concommittant g factor significantly different from 1.

V. CONCLUSIONS

The literature on the properties of dimethylsulphoxide liquid frequently refer to the fact that the liquid is "highly associated."[1] The precise meaning of this term is not quantified, but more recent conclusions based on computer simulations[20,21] and diffraction experiments[18,19] support the view that while orientational correlations certainly occur in the liquid, the extent to which it can be regarded as "associated" is still not clear. The present work, which has used a combined approach involving neutron diffraction with hydrogen isotope substitution and computer simulation, has found that some important thermodynamic quantities and experimental pair correlation functions can be well reproduced by one or another molecular force field generated from a combination of Lennard-Jones atom–atom interactions on the sulfur, oxygen, and carbon sites together with charges on some atomic sites to represent the charge distribution of this molecule. On the basis of the present computer simulation and experimental results, there is little evidence for a strong preference for particular molecular orientations, unlike the case of water, which is known to be associated and which also has a set of highly characteristic site–site correlation functions in the liquid state.

One of the previous x-ray studies presents a table of intermolecular distances,[18] but makes no mention of the difficulty of assigning individual distances from a diffraction pattern which consists of several site–site correlation

functions combined together. Previous simulations[20,21] have alluded to the sharpness of the nearest-neighbor CO peak as indicating the presence of a weak O–methyl group hydrogen bond, without considering the possible effects of hard core packing. The present work suggests that at least part of that sharpness can be attributed to packing effects around the rather distinctive shape of the DMSO molecule. There is a large dipole moment, located almost completely in the SO group of the molecule,[33,34] and the electrostatic interactions do play a role in structuring the fluid. The present results, however, do indicate that DMSO has no highly specific and powerful forces such as hydrogen bonds in water or methanol. This is borne out by the fact that correlation functions which involve the hydrogen atom, both experimentally and from computer simulation, have none of the signatures that might be expected of associates with a well-defined structure.

The potentials that have been presented in this paper show good agreement with the neutron diffraction data, but there are still some discrepancies to be understood. The data themselves have an intrinsic uncertainty which is hard to estimate because of the large number of overlapping distances in the different correlation functions, and because of the large intramolecular contributions which must be subtracted before any intermolecular functions can be determined. We derive some confidence from the present data because they do predict a molecular geometry which is in close agreement with other determinations.

From the point of view of trying to ascertain which of the present potentials is the most appropriate for simulation work, then the RS potential shows slightly better agreement with the present XX composite partial structure factor data, but it does not give an accurate heat of vaporization. The *P2* potential has the correct heat of vaporization and shows only slightly worse agreement with the neutron derived g_{XX} function. Both potentials show good agreement with the measured HH and XH functions. It remains to be seen whether a new simulation involving a revised potential can improve on the agreement seen here. The existing potentials should also be tested against dynamical data on the liquid, such as the self-diffusion coefficient and reorientational correlation times. However, a perfect match of both, i.e., important thermodynamic properties *and* structure, is probably not possible with the class of models we have used here in which many-body polarization effects are neglected. In the case of water, e.g., inclusion of many-body polarization forces has a fairly large effect on water structure.[50,51] Equivalent polarizable potential models for DMSO have not yet been explored, but would provide the likely route to improving the existing potentials. For practical purposes of simulating DMSO in concentrated mixtures, such as in DMSO–water solutions,[21,24] it appears that the structural results are rather insensitive to whether either RS, *P1*, or *P2* potentials are used, even though these potentials clearly do not give equally good results in the pure liquid.

Nothing can yet be said about the extent of orientational correlations in liquid DMSO. The second order orientational factor $g_2=1+\langle(N-1)P_2(\mathbf{u}_1\cdot\mathbf{u}_2)\rangle$, where P_2 is the second order Legendre polynomial, would be worth investigating in this respect. So far, the g factors for liquid DMSO have not been estimated from the simulation results.

Recently, one of us has developed an approach whereby information on site–site partial structure factors is used to estimate the orientational pair correlation function, via the standard spherical harmonic expansion, and employing image reconstruction techniques.[32] So far, this has only been attempted for linear diatomic molecules, but the generalization to more complex molecular shapes is expected to be straightforward. If this technique proves to be fruitful, it might be used on both the present experimental data and simulation results to estimate the degree of orientational correlation in either case. It is hoped to report on this analysis in a future communication.

ACKNOWLEDGMENTS

The RISM calculations were performed with the help of Joel Bader. This work was supported in part by NIH Grant No. RO1 GM37307 and ONR Grant No. N00014-92-J-1361.

[1] D. Martin and H. G. Hanthal, *Dimethyl Sulphoxide* (Wiley, New York, 1975).
[2] J. M. G. Cowie and P. M. Toporowski, Can. J. Chem. **39**, 2240 (1964).
[3] H. L. Clever and S. P. Pigott, J. Chem. Thermodyn. **3**, 221 (1971).
[4] M. F. Fox and K. P. Whittingham, J. Chem. Soc. Faraday Trans. **75**, 1407 (1974).
[5] J. Kenttammaa and J. J. Lindberg, Suom. Kemistil. B **33**, 32 (1960).
[6] G. J. Safford, P. C. Schaffer, P. S. Leung, G. F. Doebbler, G. W. Brady, and E. F. X. Lyden, J. Chem. Phys. **50**, 2140 (1969).
[7] A. Bertulozza, S. Bonora, M. A. Battaglia, and P. Monti, J. Raman Spectrosc. **8**, 231 (1979).
[8] G. Brink and M. Falk, J. Mol. Struct. **5**, 27 (1970).
[9] A. Allerhand and P. von R Schleyer, J. Am. Chem. Soc. **85**, 1715 (1963).
[10] B. C. Gordalla and M. D. Zeidler, Mol. Phys. **59**, 817 (1986); **74**, 975 (1991).
[11] T. Tukouhrio, L. Menafra, and H. H. Szmant, J. Chem. Phys. **61**, 2275 (1975).
[12] E. S. Barker and J. Jonas, J. Phys. Chem. **89**, 1730 (1985).
[13] M. Y. Doucet, F. Calmes-Perault, and M. T. Durand, C. R. Acad. Sci. **260**, 1878 (1965).
[14] E. Tommila and A. Pajunen, Suom. Kemistil. B **41**, 172 (1969).
[15] W. M. Madigsky and R. W. Warfield, J. Chem. Phys. **78**, 1912 (1983).
[16] U. Kaatze, M. Brai, F. D. Scholle, and R. Pottel, J. Mol. Liq. **44**, 197 (1990).
[17] T. Kondo, L. L. Kirschenbaum, J. Kim, and P. Riesz, J. Phys. Chem. **97**, 522 (1993).
[18] S. Itoh and H. Ohtaki, Z. Naturforsch. Teil A **42**, 858 (1987).
[19] H. Bertagnolli, E. Schultz, and P. Chieux, Ber. Bunsenges. Phys. Chem. **93**, 88 (1989).
[20] B. G. Rao and U. C. Singh, J. Am. Chem. Soc. **112**, 3803 (1990).
[21] I. I. Vaisman and M. L. Berkowitz, J. Am. Chem. Soc. **114**, 7889 (1992).
[22] D. F. Mierke and H. Kessler, J. Am. Chem. Soc. **113**, 9466 (1991).
[23] T. B. Douglas, J. Am. Chem. Soc. **70**, 2001 (1948).
[24] A. Luzar and D. Chandler, J. Chem. Phys. **98**, 8160 (1993).
[25] A. K. Soper and A. Luzar, J. Chem. Phys. **97**, 1320 (1992).
[26] A. Luzar, NATO ASI Ser. **329**, 197 (1991).
[27] A. Luzar, J. Chem. Phys. **91**, 3603 (1989).
[28] A. Luzar, in *Interaction of Water in Ionic and Nonionic Hydrates*, edited by H. Kleeberg (Springer, Berlin, 1987), p. 125.
[29] R. Thomas, C. B. Shoemaker, and K. Eriks, Acta Crystallogr. **21**, 12 (1966).
[30] M. A. Viswamitra, and K K Kannan, Nature **209**, 1016 (1966).

[31] A. K. Soper, in *Neutron Scattering Data Analysis 1990*, edited by M W Johnson (IOP, Bristol, 1990), No. 107.
[32] A. K. Soper, C. Andreani, and M. Nardone, Phys. Rev. E **47**, 2598 (1993).
[33] F. A. Cotton and R. Francis, J. Am. Chem. Soc. **82**, 2986 (1960).
[34] H. L. Schlafer and W. Scheffernicht, Angew. Chem. **72**, 618 (1960).
[35] U. C. Singh and P. A. Kollman, J. Comput. Chem. **5**, 129 (1984).
[36] P. C. Hariharan and J. A. Pople, Theor. Chim. Acta **28**, 213 (1973).
[37] S. Nosé, J. Chem. Phys. **81**, 511 (1989).
[38] W. G. Hoover, Phys. Rev. A **31**, 1695 (1985).
[39] M. P. Allen and D. J. Tildesley, *Computer Simulation of Liquids* (Clarendon, Oxford, 1987).
[40] Three molecular dynamics simulations have recently been carried out (Refs. 20–22) using the same force field model for DMSO, namely, the Rao–Singh (RS) (Ref. 20) potential. The complete set of the correct atom–atom pair distribution functions has not been reported in any of these works. Specifically, Rao and Singh (Ref. 20) do not report a split in the first intermolecular peak in $g_{OS}(r)$, as was observed by Vaisman and Berkowitz (Ref. 21) and in the present simulation. Merke and Kessler (Ref. 22) claimed that their $g(r)$'s agreed with those of Ref. 20, but they do not show the data.
[41] A. K. Soper and P. A. Egelstaff, Mol. Phys. **42**, 399 (1981).
[42] A. K. Soper and R. N. Silver, Phys. Rev. Lett. **49**, 471 (1982).
[43] D. Chandler, J. D. Weeks, and H. C. Andersen, Science **220**, 787 (1983).
[44] D. Chandler, *Studies in Statistical Mechanics 8*, edited by J. L. Lebowitz and E. N. Montroll (North–Holland, Amsterdam, 1992).
[45] J. G. Kirkwood, J. Chem. Phys. **7**, 911 (1939).
[46] H. Frohlich, *Theory of Dielectrics* (Oxford University, Oxford, 1993).
[47] J. P. Hansen and I. R. McDonald, *Theory of Simple Liquids*, 2nd ed. (Academic, New York, 1990), p. 462.
[48] J. F. Castel and P. G. Sears, J. Chem. Eng. Data **19**, 196 (1974).
[49] A. Luzar, J. Mol. Liq. **46**, 221 (1990).
[50] H. J. C. Berendsen, J. R. Grigera, and T. P. Straatsma, J. Phys. Chem. **91**, 6269 (1987).
[51] P. Ahlström, A. Wallqvist, S. Engström, and Bo Jönsson, Mol. Phys. **68**, 563 (1989).